New Tikhonov Regularization for Blind Image Restoration

Yuying Shi[1(✉)], Qiao Liu[1], and Yonggui Zhu[2]

[1] Department of Mathematics and Physics, North China Electric Power University, Beijing 102206, China
yyshi@ncepu.edu.cn
[2] School of Science, Communication University of China, Beijing 100024, China

Abstract. Blind image restoration is a challenging problem with unknown blurring kernel. In this paper, we propose a new algorithm based on a new Tikhonov regularization term, which combines three techniques including the split Bregman technique, fast Fourier transform and spectral decomposition technology to accelerate the computation process. Numerical results demonstrate that the proposed algorithm is simple, fast and effective for blind image restoration.

1 Introduction

Blind image restoration has been widely applied in remote sensing, astronomy, medical imaging, video cameras and so on (see, e.g. [8,10,18]). For example, when taking the photograph of a moving object, the shutter speed and the speed of the object are unknown. The process of degradation can be modeled as: $g = h*f+n$, where g stands for the degraded image, f represents the original image, h is the blurring kernel (also called as point spread function (PSF)), n expresses the noise, and $*$ denotes convolution operation. As the PSF is unknown, a lot of restoration techniques have been proposed (see, e.g. [1,3,5,11–14,16,17,19,26]). It is becoming one of the most challenging problems for its complication and difficulty.

Regularization is one way to avoid the problems due to the ill-posed nature of blind image restoration. You and Kaveh [26] used the minimizing formulation with H^1 regularization terms for both the image and the PSF:

$$\min_{f,h}\left\{\frac{1}{2}\|h*f-g\|_2^2+\lambda_1\|f\|_{H^1}^2+\lambda_2\|h\|_{H^1}^2\right\}. \tag{1}$$

Chan and Wong [5] regularized both the image and the PSF by the famous total variation (TV) regularization terms (see, e.g. [5,21]) instead of the H^1-norm:

$$\min_{f,h}\left\{\frac{1}{2}\|h*f-g\|_2^2+\lambda_1 TV(f)+\lambda_2 TV(h)\right\}. \tag{2}$$

The TV regularization is considered to be one of the best approaches to recovering edges of image, but also one of the hardest to computing because

Y. Zhao et al. (Eds.): ICIG 2017, Part III, LNCS 10668, pp. 113–123, 2017.
https://doi.org/10.1007/978-3-319-71598-8_11

of the nonlinearity and non-differentiability of the TV regularization term. The split Bregman (SB) method is shown to be efficient to handle the TV term with notable stability and fast convergence rate (see, e.g. [4,5,7,9]). Based on the SB method, the minimization problem can be divided into several subproblems. The important and difficult subproblems are to effectively find the solutions f and h alternatively, so we need to solve large linearized systems of equations. To solve large equations, the cosine preconditioned conjugate gradient method and the fixed-point method are proposed in [5]. Coupled systems of f and h are evolved by a time marching method, which is based on the gradient descent method [9]. Chang et al. [25] applied an algebraic multigrid (AMG) method and Krylov subspace acceleration technique to solve the linearized systems of equations [25]. We also noticed that the 2D fast Fourier transform (FFT) [4,14] is fast and simple. Moreover, the spectral decomposition technology (SDT) [24] is efficient for handling a new Tikhonov regularization term [6,15]. The SDT not only reduces the amount of calculation, but also saves the storage space.

The purpose of this paper is to briefly describe a combined algorithm of the SB method, FFT and SDT, which agglomerates advantages of the above three methods, and realize blind image restoration with a TV regularization term and a new Tikhonov regularization term.

The organization of this paper is given as follows. Section 2 exhibits our new combined algorithm based on the SB method, FFT and SDT. Computational results are shown in Sect. 3. Finally, some conclusions are given in Sect. 4.

2 Proposed Algorithm

In this section, we propose a fast combined algorithm to solve blind image restoration problem with the TV regularization term for h and the new Tikhonov (NT) regularization term for f [6] using the SB technique, FFT and SDT. We denote the proposed algorithm as NT-SB algorithm.

2.1 NT-SB Algorithm

To induce our new algorithm, we need to modify the model (2) as follows:

$$\min_{f,h}\left\{\frac{1}{2}\|h*f-g\|_2^2+\frac{\lambda_1}{2}\|L_\lambda f\|_2^2+\lambda_2\sum_i\sqrt{(\nabla_x h)_i^2+(\nabla_y h)_i^2}\right\}, \tag{3}$$

where $\lambda_1,\lambda_2>0$ are regularization parameters, $\|L_\lambda f\|_2^2$ is a regularization term, which can filter high frequency information such as noise. We will show the detailed definition of L_λ in (12) later.

Introducing two auxiliary variables c_1, c_2 similar to [7], we make the following substitutions for the model (2), $\nabla_x h \to c_1, \nabla_y h \to c_2$. This yields the following equivalent constrained problem:

$$\begin{aligned}&\min_{f,h,c_1,c_2}\left\{\frac{1}{2}\|h*f-g\|_2^2+\frac{\lambda_1}{2}\|L_\lambda f\|_2^2+\lambda_2\|(c_1,c_2)\|_2\right\},\\ &s.t.\quad \nabla_x h=c_1,\nabla_y h=c_2.\end{aligned} \tag{4}$$

Notice that here we only need two auxiliary variables, since there is only one TV regularization term. While for the following TV-SB algorithm in Sect. 3, we have to introduce four variables.

Thus the iterative scheme of our new algorithm based on the SB technique is as follows:

$$\begin{aligned}&(f^{k+1}, h^{k+1}, c_1^{k+1}, c_2^{k+1}) = \\ &arg\min_{f,h,c_1,c_2}\Big\{\frac{1}{2}\|h*f-g\|_2^2 + \frac{\lambda_1}{2}\|L_\lambda f\|_2^2 + \lambda_2\|(c_1,c_2)\|_2 \\ &+\frac{\gamma_2}{2}(\|c_1-\nabla_x h - s_1^k\|_2^2 + \|c_2-\nabla_y h - s_2^k\|_2^2)\Big\},\end{aligned} \tag{5}$$

and

$$\begin{aligned}s_1^{k+1} &= s_1^k + \nabla_x h^{k+1} - c_1^{k+1},\\ s_2^{k+1} &= s_2^k + \nabla_y h^{k+1} - c_2^{k+1},\end{aligned} \tag{6}$$

where the parameters $\lambda_1, \lambda_2 > 0$ fit the fidelity term and the regularization terms, $\gamma_2 > 0$ regulates the penalty function terms. The minimization problem (5) can also be decoupled into the following subproblems:

1: h-subproblem: for fixed $f^k, c_1^k, c_2^k, s_1^k, s_2^k$, we need to solve

$$h^{k+1} = arg\min_h\Big\{\mathcal{H}(h) + \frac{\gamma_2}{2}(\|c_1^k - \nabla_x h - s_1^k\|_2^2 + \|c_2^k - \nabla_y h - s_2^k\|_2^2)\Big\}, \tag{7}$$

where $\mathcal{H}(h) = \frac{1}{2}\|f^k * h - g\|_2^2$.
According to the optimality condition, which requires us to solve

$$\begin{aligned}&(f^k)^T * (f^k * h^{k+1} - g) + \gamma_2\nabla^T\nabla h^{k+1}\\ &+\gamma_2(\nabla_x^T(s_1^k - c_1^k) + \nabla_y^T(s_2^k - c_2^k)) = 0.\end{aligned} \tag{8}$$

That is,

$$h^{k+1} = \mathcal{F}^{-1}\Big[\frac{\mathcal{F}((f^k)^T g + \gamma_2(\nabla_x^T(c_1^k - s_1^k) + \nabla_y^T(c_2^k - s_2^k))}{\mathcal{F}((f^k)^T f^k - \gamma_2\triangle)}\Big], \tag{9}$$

where $\nabla^T\nabla = -\triangle, \nabla^T = -div$.

2: f-subproblem: for fixed h^{k+1}, we need to solve

$$f^{k+1} = arg\min_f\Big\{\mathcal{F}_1(f) + \mathcal{F}_2(f)\Big\}, \tag{10}$$

where $\mathcal{F}_1(f) = \frac{1}{2}\|\tilde{H}f - g\|_2^2$, $\mathcal{F}_2(f) = \frac{\lambda_1}{2}\|L_\lambda^{k+1} f\|_2^2$, and $\tilde{H}$ is the BCCB (Block Circulant with Circulant Blocks) blur matrix got by the blurring kernel h with periodic boundary conditions [20,22]. We apply the spectral decomposition technology for the blurring matrix $\tilde{H}$, and have

$$\tilde{H} = F^*\Sigma F, \tag{11}$$

where F is a 2D unitary discrete Fourier transform (DFT) matrix, the conjugate transpose of a complex matrix F, denoted F^* and the diagonal matrix $\Sigma = diag[\hat{\sigma}_1, \hat{\sigma}_2, \cdots, \hat{\sigma}_n]$ (see, e.g. [6]), where $\hat{\sigma}_1, \hat{\sigma}_2, \cdots, \hat{\sigma}_n$ are eigenvalues of $\tilde{H}$. Construct the regularization matrix L_λ as:

$$L_\lambda = D_\lambda F, \tag{12}$$

where

$$D_\lambda^2 = \begin{pmatrix} \max(\lambda^2 - \hat{\sigma}_1^2, 0) & & & \\ & \max(\lambda^2 - \hat{\sigma}_2^2, 0) & & \\ & & \ddots & \\ & & & \max(\lambda^2 - \hat{\sigma}_n^2, 0) \end{pmatrix}. \tag{13}$$

According to the NT method proposed in [15], we have

$$f = F^*(\hat{\sigma}^*\hat{\sigma} + \lambda_1 (D_\lambda^{k+1})^* D_\lambda^{k+1})^{-1} \hat{\sigma}^* F g. \tag{14}$$

3: c_1, c_2-subproblems: for fixed f^{k+1} and h^{k+1}, we need to solve

$$\begin{aligned} (c_1^{k+1}, c_2^{k+1}) = arg \min_{c_1, c_2} \Big\{ & \lambda_2 \|(c_1, c_2)\|_2 \\ & + \frac{\gamma_2}{2} (\|c_1 - \nabla_x h^{k+1} - s_1^k\|_2^2 + \|c_2 - \nabla_y h^{k+1} - s_2^k\|_2^2) \Big\}. \end{aligned} \tag{15}$$

By shrinkage formulation (see, e.g. [7,23]), the solutions of (15) are

$$\begin{aligned} c_1^{k+1} &= \frac{\nabla_x h^{k+1} + s_1^k}{W^k} \max\{W^k - \frac{\lambda_2}{\gamma_2}, 0\}, \\ c_2^{k+1} &= \frac{\nabla_y h^{k+1} + s_2^k}{W^k} \max\{W^k - \frac{\lambda_2}{\gamma_2}, 0\}, \end{aligned} \tag{16}$$

where $W^k = \sqrt{(\nabla_x h^{k+1} + s_1^k)^2 + (\nabla_y h^{k+1} + s_2^k)^2}$.

We summarize the NT-SB algorithm as follows:

NT-SB Algorithm

1. Initializing $f^0, c_1^0, c_2^0, s_1^0, s_2^0$,
2. While $\|f^{k+1} - f^k\|_2 / \|f^k\|_2 > tol$, do
   a: solve (9) to get h^{k+1},
   b: solve (14) to get f^{k+1},
   c: solve (16) to get c_1^{k+1}, c_2^{k+1},
   d: update s_1^{k+1}, s_2^{k+1} by (6).
   end do

Here, *tol* denotes the tolerance value for iteration scheme, and the order of the h and f subproblems can not be transposed.

3 Experimental Results

To show the superiority of the proposed algorithm, we compare the NT-SB algorithm with the TV-SB algorithm that solves the original model (2) using split Bregman method. First, we simply show the TV-SB algorithm. Using several auxiliary variables b_1, b_2, c_1, c_2, we need to solve the following equivalent constrained problem:

$$\begin{aligned} &\min_{\substack{f,h,b_1,b_2\\c_1,c_2}} \left\{ \tfrac{1}{2}\|h * f - g\|_2^2 + \lambda_1 \|(b_1, b_2)\|_2 + \lambda_2 \|(c_1, c_2)\|_2 \right\}, \\ &s.t. \quad \nabla_x f = b_1, \nabla_y f = b_2, \nabla_x h = c_1, \nabla_y h = c_2. \end{aligned} \tag{17}$$

For the h-subproblem, we can get the same solution (9). For the f-subproblem, we get

$$f^{k+1} = \mathcal{F}^{-1}[\frac{\mathcal{F}((h^{k+1})^T g + \gamma_1(\nabla_x^T(b_1^k - t_1^k) + \nabla_y^T(b_2^k - t_2^k))}{\mathcal{F}((h^{k+1})^T h^{k+1} - \gamma_1 \triangle)}]. \tag{18}$$

By shrinkage formulation as above, we obtain

$$\begin{aligned} b_1^{k+1} &= \frac{\nabla_x f^{k+1} + t_1^k}{V^k} \max\{V^k - \frac{\lambda_1}{\gamma_1}, 0\}, \\ b_2^{k+1} &= \frac{\nabla_y f^{k+1} + t_2^k}{V^k} \max\{V^k - \frac{\lambda_1}{\gamma_1}, 0\}, \\ c_1^{k+1} &= \frac{\nabla_x h^{k+1} + s_1^k}{W^k} \max\{W^k - \frac{\lambda_2}{\gamma_2}, 0\}, \\ c_2^{k+1} &= \frac{\nabla_y h^{k+1} + s_2^k}{W^k} \max\{W^k - \frac{\lambda_2}{\gamma_2}, 0\}, \end{aligned} \tag{19}$$

where

$$\begin{aligned} V^k &= \sqrt{(\nabla_x f^{k+1} + t_1^k)^2 + (\nabla_y f^{k+1} + t_2^k)^2}, \\ W^k &= \sqrt{(\nabla_x h^{k+1} + s_1^k)^2 + (\nabla_y h^{k+1} + s_2^k)^2}. \end{aligned}$$

And the iterative parameters

$$\begin{aligned} t_1^{k+1} &= t_1^k + \nabla_x f^{k+1} - b_1^{k+1}, \\ t_2^{k+1} &= t_2^k + \nabla_y f^{k+1} - b_2^{k+1}, \\ s_1^{k+1} &= s_1^k + \nabla_x h^{k+1} - c_1^{k+1}, \\ s_2^{k+1} &= s_2^k + \nabla_y h^{k+1} - c_2^{k+1}. \end{aligned} \tag{20}$$

We summarize the TV-SB algorithm as follows:

TV-SB Algorithm

1. Initializing $f^0, b_1^0, b_2^0, t_1^0, t_2^0, c_1^0, c_2^0, s_1^0, s_2^0$,
2. While $\|f^{k+1} - f^k\|_2 / \|f^k\|_2 > tol$, do
   a: solve (9) to get h^{k+1},
   b: solve (18) to get f^{k+1},
   c: solve (19) to get $b_1^{k+1}, b_2^{k+1}, c_1^{k+1}, c_2^{k+1}$,
   d: update $t_1^{k+1}, t_2^{k+1}, s_1^{k+1}, s_2^{k+1}$ by (20).
   end do

Some remarks are in order.

(a) Comparing with the TV-SB algorithm, our proposed NT-SB algorithm uses less variables (missing b_1, b_2, t_1, t_2) and less initial values need to be set (missing $b_1^0, b_2^0, t_1^0, t_2^0$).
(b) It is seen that, the computational complexity is obviously reduced for steps c and d.

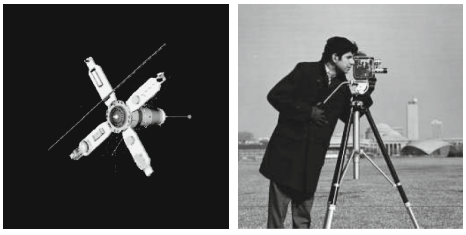

(a) (b)

Fig. 1. Original Images

Table 1. $ISNR$ values and computing times using the TV-SB algorithm and the NT-SB algorithm with different Gaussian Blurs (GB) and Moffat Blurs (MB).

Blur(kernel size)	Algorithm	Iteration	Time(s)	$ISNR$
GB (20)	TV-SB	100	34.1719	1.4910
	NT-SB	40	23.8906	2.2532
MB (20)	TV-SB	44	16.0625	0.8769
	NT-SB	24	14.4063	1.3146
GB (30)	TV-SB	100	34.1719	1.4910
	NT-SB	40	23.8906	2.2532
MB (30)	TV-SB	45	17.2969	0.8717
	NT-SB	23	13.8281	1.1383

(a) GB: 20×20 (b) TV-SB (c) NT-SB

(d) GB: 30×30 (e) TV-SB (f) NT-SB

(g) MB: 20×20 (h) TV-SB (i) NT-SB

(j) MB: 30×30 (k) TV-SB (l) NT-SB

Fig. 2. Comparisons of the TV-SB algorithm and the NT-SB algorithm. Column 1: Blurred images contaminated by different blurs with different blurring kernel sizes with the variance of $\sigma^2 = 1$; Column 2: Restored images by the TV-SB algorithm; Column 3: Restored images by the NT-SB algorithm.

In this section, we test two gray images (satellite and cameraman images) in Fig. 1 which are both of size 256×256 pixels to show the effectiveness and feasibility of the TV-SB algorithm and the NT-SB algorithm. In the following examples, we mainly compare the visual quality of the restored images and the improvement in signal to noise ratio ($ISNR$) value [2]. The larger the $ISNR$ value is, the better the restored result is.

The elements of the noise vector n are normally distributed with zero mean, and the standard deviation is chosen such that $\frac{\|n\|_2}{\|g\|_2} = 0.01$. In this case, we say that the level of noise is 1%. Moreover, the numerical examples are all implemented with MATLAB (R2010a) and the computer of test has 1G RAM and Intel(R) Pentium(R) D CPU @2.80 GHz.

Table 2. $ISNR$ values and computing times using the TV-SB algorithm and the NT-SB algorithm with different Gaussian Blurs (GB) and Moffat Blurs (MB) and 1% Gaussian noise.

Blur	Algorithm	Iteration	Time(s)	$ISNR$
GB ($\sigma^2 = 1$)	TV-SB	50	18.8125	1.4161
	NT-SB	20	12.0625	1.6982
MB ($\sigma^2 = 1$)	TV-SB	50	18.2969	1.3533
	NT-SB	15	9.4844	1.4057
GB ($\sigma^2 = 1.5$)	TV-SB	50	17.8438	0.7389
	NT-SB	20	12.4375	0.8107
MB ($\sigma^2 = 1.5$)	TV-SB	50	17.1719	0.8776
	NT-SB	15	8.7500	0.8971

Then, to compare the properties of the TV-SB algorithm and the NT-SB algorithm, we consider the degraded images contaminated by Gaussian or Moffat blur and Gaussian noise.

First of all, we consider the cameraman image contaminated by only Gaussian or Moffat blur, the restored images are shown in Fig. 2. The parameters in the algorithms are set to be $\lambda_1 = 13, \lambda_2 = 0.1, \gamma_1 = 0.1e-6, \gamma_2 = 0.2$. Blurred images contaminated by the size of 20×20 and 30×30 Gaussian blurs with $\sigma^2 = 1$ are displayed in Figs. 2(a) and (d), blurred images contaminated by the size of 20×20 and 30×30 Moffat blurs with $\sigma^2 = 1$ are depicted in Figs. 2(g) and (j); restored images by the TV-SB and NT-SB algorithms are shown in the second and third columns of Fig. 2, respectively. The $ISNR$ values, number of iterations and computing times are listed in Table 1. We can see that the NT-SB algorithm has better restoration effect with larger $ISNR$ values and needs fewer number of iterations and fewer computing times (cf. Table 1).

Next, we consider the blurred-noisy satellite image contaminated by Gaussian or Moffat blur and 1% Gaussian noise in Fig. 3. Since the background color of satellite image is black, the noise is not so obvious in the contaminated images

(a) GB: $\sigma^2 = 1$ (b) TV-SB (c) NT-SB

(d) GB: $\sigma^2 = 1.5$ (e) TV-SB (f) NT-SB

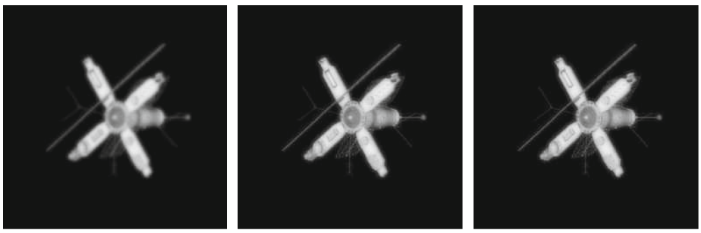

(g) MB: $\sigma^2 = 1$ (h) TV-SB (i) NT-SB

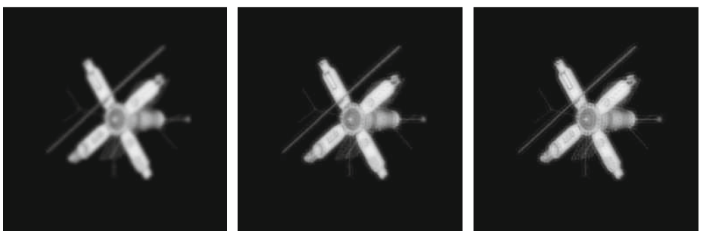

(j) MB: $\sigma^2 = 1.5$ (k) TV-SB (l) NT-SB

Fig. 3. Comparisons of the TV-SB algorithm and the NT-SB algorithm. Column 1: Blurred-Noisy images contaminated by 10×10 Gaussian or Moffat blur with different ambiguous degrees and noise of 1%; Column 2: Restored images by the TV-SB algorithm; Column 3: Restored images by the NT-SB algorithm.

(the first column of Fig. 3). The parameters in the algorithms are set to be $\lambda_1 = 1, \lambda_2 = 0.05, \gamma_1 = 0.1e-4, \gamma_2 = 8$. Blurred-noisy images contaminated by Gaussian and Moffat Blurs with $\sigma^2 = 1$ and 1% Gaussian noise are exemplified in Figs. 3(a) and (g), respectively, blurred-noisy images contaminated by the size of 10×10 Gaussian and Moffat Blurs with $\sigma^2 = 1.5$ and 1% Gaussian noise are exemplified in Figs. 3(d) and (j), respectively; restored images by the TV-SB and NT-SB algorithms are shown in the second and third columns of Fig. 3. We tabulate the $ISNR$ values, number of iterations and computing times of the two algorithms in Table 2, which shows that the NT-SB algorithm has almost the same $ISNR$ values as the TV-SB algorithm, but the NT-SB algorithm needs less number of iterations and fewer computing times (see Table 2).

By observing Figs. 2 and 3, the NT-SB algorithm behaves better for the blurred-noisy images in visual and faster than the TV-SB algorithm with the same parameters.

4 Conclusions

In this paper, we introduced a new Tikhonov regularization term to replace the TV regularization term for blind restoration problem, and applied the split Bregman technique to separate the minimum formulation with the TV regularization term for the blurring kernel and the new Tikhonov regularization term for the image into several subproblems. In the process of solving the subproblems, we combined the FFT and the SDT to accelerate the computation. The TV-SB and NT-SB algorithms were shown to be effective by several numerical experiments. The NT-SB algorithm needed less space, fewer number of iterations, shorter computing times and better restored effect comparing with the TV-SB algorithm.

Acknowledgments. The authors wish to thank the referees for many constructive comments which lead to a great improvement of the paper. This research is supported by NSFC grants (No. 11271126, 11571325).

References

1. Ayers, G.R., Dainty, J.C.: Iterative blind deconvolution method and its applications. Opt. Lett. **13**(7), 547–549 (1988)
2. Babacan, S.D., Molina, R., Katsaggelos, A.K.: Total variation image restoration and parameter estimation using variational posterior distribution approximation. In: IEEE International Conference on Image Processing 2007, ICIP 2007, vol. 1, pp. 1–97. IEEE (2007)
3. Biemond, J., Tekalp, A.M., Lagendijk, R.L.: Maximum likelihood image and blur identification: a unifying approach. Opt. Eng. **29**(5), 422–435 (1990)
4. Chan, R.H., Tao, M., Yuan, X.M.: Constrained total variation deblurring models and fast algorithms based on alternating direction method of multipliers. SIAM J. Imaging Sci. **6**(1), 680–697 (2013)

5. Chan, T.F., Wong, C.-K.: Total variation blind deconvolution. IEEE Trans. Image Process. **7**(3), 370–375 (1998)
6. Fuhry, M., Reichel, L.: A new tikhonov regularization method. Numer. Algorithms **59**(3), 433–445 (2012)
7. Goldstein, T., Osher, S.: The split bregman method for l1-regularized problems. SIAM J. Imaging Sci. **2**(2), 323–343 (2009)
8. Hansen, P.C., Nagy, J.G., O'leary, D.P.: Deblurring Images: Matrices, Spectra, and Filtering, vol. 3. Siam (2006)
9. He, L., Marquina, A., Osher, S.J.: Blind deconvolution using TV regularization and bregman iteration. Int. J. Imaging Syst. Technol. **15**(1), 74–83 (2005)
10. Jin, C., Chen, C., Bu, J.: A new approach of blind image restoration. In: IEEE International Conference on Systems, Man and Cybernetics 2003, vol. 1, pp. 245–250. IEEE (2003)
11. Kundur, D., Hatzinakos, D.: Blind image deconvolution. IEEE Signal Process. Mag. **13**(3), 43–64 (1996)
12. Kundur, D., Hatzinakos, D.: A novel blind deconvolution scheme for image restoration using recursive filtering. IEEE Trans. Signal Process. **46**(2), 375–390 (1998)
13. Lagendijk, R.L., Biemond, J., Boekee, D.E.: Identification and restoration of noisy blurred images using the expectation-maximization algorithm. IEEE Trans. Acoust. Speech Signal Process. **38**(7), 1180–1191 (1990)
14. Li, W., Li, Q., Gong, W., Tang, S.: Total variation blind deconvolution employing split bregman iteration. J. Vis. Commun. Image Represent. **23**(3), 409–417 (2012)
15. Liu, J., Shi, Y., Zhu, Y.: A fast and robust algorithm for image restoration with periodic boundary conditions. J. Comput. Anal. Appl. **17**(3), 524–538 (2014)
16. Marquina, A.: Nonlinear inverse scale space methods for total variation blind deconvolution. SIAM J. Imaging Sci. **2**(1), 64–83 (2009)
17. McCallum, B.C.: Blind deconvolution by simulated annealing. Opt. Commun. **75**(2), 101–105 (1990)
18. Moffat, A.F.J.: A theoretical investigation of focal stellar images in the photographic emulsion and application to photographic photometry. Astron. Astrophys. **3**(1), 455 (1969)
19. Nayakkankuppam, M.V., Venkatesh, U.V.: Deblurring the gaussian blur using a wavelet transform. Pattern Recognit. **28**(7), 965–976 (1995)
20. Ng, M.K., Chan, R.H., Tang, W.C.: A fast algorithm for deblurring models with neumann boundary conditions. SIAM J. Sci. Comput. **21**(3), 851–866 (1999)
21. Rudin, L.I., Osher, S., Fatemi, E.: Nonlinear total variation based noise removal algorithms. Phys. D Nonlinear Phenom. **60**(1), 259–268 (1992)
22. Shi, Y., Chang, Q.: Acceleration methods for image restoration problem with different boundary conditions. Appl. Numer. Math. **58**(5), 602–614 (2008)
23. Shi, Y., Chang, Q.: Efficient algorithm for isotropic and anisotropic total variation deblurring and denoising. J. Appl. Math. **2013**, 14 (2013). Article ID 797239
24. Wang, Z.F., Zhang, Z.J., Li, X.M., Tang, Y.D.: An adaptive image denoising algorithm based on SVD and energy minimization. J. Image Graph. **12**(4), 603–607 (2007)
25. Xu, J., Chang, Q.: A robust algorithm for blind total variation restoration. Acta Math. Appl. Sinica Engl. Ser. **24**(4), 681–690 (2008)
26. You, Y.L., Kaveh, M.: A regularization approach to joint blur identification and image restoration. IEEE Trans. Image Process. **5**(3), 416–428 (1996)